Thermal Stability Study of BaAl2Si2O8:Eu2+ Phosphor Using Its Polymorphism for Plasma Display Panel Application

3 AUTHORS, INCLUDING:

Won Bin Im
Chonnam National University
85 PUBLICATIONS   1,850 CITATIONS

SEE PROFILE

Thermal Stability Study of BaAl$_2$Si$_2$O$_8$:Eu^{2+} Phosphor Using Its Polymorphism for Plasma Display Panel Application

Won Bin Im,[†] Yong-Il Kim,[‡] and Duk Young Jeon*,[†]

Department of Materials Science and Engineering, Korea Advanced Institute of Science and Technology, Daejeon 305-701, Republic of Korea, and Korea Research Institute of Standards and Science, P.O. Box 102, Yuseong, Daejeon 305-600, Republic of Korea

We have evaluated the thermal stability of BaAl$_2$Si$_2$O$_8$:Eu^{2+} (BAS:Eu^{2+}) phosphor using its polymorph property and hexagonal and monoclinic crystal structure, depending upon firing temperature for plasma display panel application. When BAS:Eu^{2+} samples having each characteristic crystal structure were baked at 500 °C in air for 30 min, the baked monoclinic BAS:Eu^{2+} showed the same photoluminescence (PL) intensity as the fresh one, whereas the baked hexagonal one lost its PL intensity significantly, corresponding to about 34%. From analyses of electron spin resonance on Eu^{2+} and Rietveld refinement, the difference of thermal stability between hexagonal and monoclinic BAS:Eu^{2+} could be ascribed to both the crystal structure of host materials and the average interatomic distances between the Eu^{2+} ion and oxygen which plays the key role of shield for Eu^{2+} ions against an oxidation atmosphere.

1. Introduction

In recent years, plasma display panels (PDPs) have been frequently used for home theater or a large-screen wall-attached televisions as a result of their wide view angle, good image quality, and low cost. However, there are some issues that need to be improved in terms of luminous efficiency and lifetime which are directly related to the performance of phosphors used in PDPs. Among the phosphors used for PDPs applications, BaMgAl$_{10}$O$_{17}$:Eu^{2+} (BAM), most frequently used as a blue phosphor, has received attentions because it is considerably less stable than the red or the green counterpart. Thanks to many researchers' studies about the stability of BAM, it has been found that the degradation process is caused by several paths such as thermal treatment during PDP manufacturing, irradiation by vacuum ultraviolet (VUV) photons (<200 nm), and ion sputtering. Among them, the thermal degradation during the manufacturing process is regarded as a particularly serious problem which is probably related with either change in valance of Eu^{2+} to Eu^{3+} or in the crystal structure of BAM (β-alumina).[1−9]

As mentioned above, thermal stability of phosphors during the burn-out of binder after applying phosphor paste in the manufacturing of PDPs has been the most important factor demanded for color emitting phosphors. Because such a baking process often uses temperatures of up to 500 °C, it has a large effect on the photoluminescence (PL) properties of phosphors.[7,10−12]

Recently, CaMgSi$_2$O$_6$:Eu^{2+} (CMS:Eu^{2+}, monoclinic) has been studied as a new promising blue PDP phosphor because it is thermally more stable than BAM.[2,13,14] The origin of its enhanced thermal stability was not clarified. In addition, it is difficult to compare BAM with CMS:Eu^{2+} in terms of thermal stability during the baking process because these two phosphors have different chemical compositions. Meanwhile, we have wondered whether the crystal structure of a host lattice has any influence on thermal stability. To shed some light on the influence of a crystal structure on thermal stability of PDP phosphors, we have selected BaAl$_2$Si$_2$O$_8$:Eu^{2+} (BAS:Eu^{2+}) phosphor, which has polymorphism such as hexagonal or monoclinic structure depending upon firing temperatures.[15] By utilizing the polymorph of BAS:Eu^{2+}, we can successively exclude contributions of differences in chemical compositions when evaluating thermal stability.

In this study, we have synthesized a single hexagonal and monoclinic phase of BAS:Eu^{2+} and evaluated their thermal

* To whom correspondence should be addressed. Fax: +82-42-869-3310. Tel.: +82-42-869-3337. E-mail: dyj@kaist.ac.kr.
† Korea Advanced Institute of Science and Technology.
‡ Korea Research Institute of Standards and Science.

(1) Oshio, S.; Matsuoka, T.; Tanaka, S.; Kobayashi, H. *J. Electrochem. Soc.* **1998**, *145* (11), 3903.
(2) Kunimoto, T.; Yoshimatsu, R.; Hhmi, K.; Tanaka, S.; Kobayashi, H. *IEICE Trans. Electron.* **2002**, *E85-C*, 11.
(3) Dawson, B.; Ferguson, M.; Marking, G.; Diaz, A. L. *Chem. Mater.* **2004**, *16*, 5311.
(4) Boolchand, P.; Mishra, K. C.; Raukus, M.; Ellens, A.; Schmidt, P. C. *Phys. Rev. B* **2002**, *66*, 134429.
(5) Kim, K.-B.; Kim, Y.-I.; Chun, H.-G.; Cho, T.-Y.; Jung, J.-S.; Kang, J.-G. *Chem. Mater.* **2002**, *14*, 5045.
(6) Kim, Y.-I.; Kim, K.-B.; Jung, M.-J.; Hong, J.-S. *J. Lumin.* **2002**, *99*, 91.
(7) Zhang, S.; Kono, T.; Ito, A.; Yasaka, T.; Uchiike, H. *J. Lumin.* **2004**, *106*, 39.
(8) Jung, K. Y.; Lee, H. Y.; Kang, Y. C.; Park, S. B.; Yang, Y. S. *Chem. Mater.* **2005**, *17*, 2729.
(9) Im, W. B.; Kim, Y.-I.; Kang, J. H.; Jeon, D. Y. *Solid State Commun.* **2005**, *134*, 177.
(10) Sohn, K. S.; Kim, S. S.; Park, H. D. *Appl. Phys. Lett.* **2002**, *81*, 10, 1759.
(11) Do, Y. R.; Park, D. H.; Kim, Y. S. *J. Eletrochem. Soc.* **2004**, *151* (10), H210.
(12) Kim, K.-B.; Koo, K.-W.; Cho, T.-Y.; Chun, H.-G. *Mater. Chem. Phys.* **2003**, *80*, 682.
(13) Im, W. B.; Kang, J. H.; Lee, D. C.; Lee, S.; Jeon, D. Y.; Kang, Y. C.; Jung, K. Y. *Solid State Commun.* **2005**, *133*, 197.
(14) Im, W. B.; Kim, Y.-I.; Jeon, D. Y. *J. Mater. Res.* **2005**, *20* (8), 2061.
(15) Lin, H. C.; Foster, W. R. *Am. Mineral.* **1968**, *53*, 134.

BaAl₂Si₂O₈:Eu²⁺ Phosphor Thermal Stability Study

Chem. Mater., Vol. 18, No. 5, 2006 1191

stability. Furthermore, this study suggests a criterion of selection of host lattices for a PDP blue-emitting phosphor from a point of view of thermal stability during the baking process.

2. Experimental Section

The samples of each polymorph BAS:Eu^{2+} were prepared by a solid-state reaction using $BaCO_3$ (Aldrich, 99.9%), Al_2O_3 (Sumitomo, 99.99%), SiO_2 (Kojundo, 99.9%), and EuF_3 (Aldrich, 99.99%) as starting materials fired between 1300 and 1400 °C in a reducing atmosphere for 3 h. To investigate the effect of the baking process, the samples were baked at 500 °C in air for 30 min. The emission spectra of polymorph BAS:Eu^{2+} were acquired using a standard spectrometer setup from DARSA PRO PL System (Professional Scientific Instrument Co., Korea), which utilizes a deuterium lamp as the excitation source. The sample chamber was maintained at about 5×10^{-5} Torr using a turbo pumping system. PL spectra were obtained by scanning a wavelength region from 300 to 700 nm under an excitation of 147 nm radiation from the deuterium lamp at room temperature. The electron spin resonance (ESR, JES-FA200) measurements at room temperature were carried out at X-band frequency to observe the behavior of Eu^{2+} ions. The X-ray diffraction (XRD) data were obtained over the scattering angle range of $10 \leq 2\theta \leq 130°$ at a step of 0.02° using Cu Kα radiation (Rigaku Dmax2200V). The Rietveld refinement against XRD data was made with the General Structure Analysis System (GSAS) program.[16] The experimental diffraction profiles were modeled by a pseudo-Voigt function within GSAS.[17]

3. Results and Discussion

We have synthesized single hexagonal and monoclinic phases of BAS:Eu^{2+} between 1300 and 1400 °C successfully. Their XRD patterns agree well with JCPDS 38-1450 and 28-0124, which correspond to monoclinic and hexagonal BAS, respectively. According to Lin and Forster's reports about polymorphism of BAS,[15] there are four polymorphs of BAS (viz., paracelsian, orthorhombic, hexagonal, and monoclinic form). Among existed polymorphs of BAS, we were able to synthesize both hexagonal and monoclinic BAS of a single phase by changing the firing temperature.

The emission spectra of the polymorph BAS:Eu^{2+}, monoclinic (M-BAS:Eu^{2+}) and hexagonal BAS:Eu^{2+} (H-BAS:Eu^{2+}), under a 147 nm excitation source are shown in Figure 1. In the PL spectra, the emission peaks of M-BAS:Eu^{2+} and H-BAS:Eu^{2+} were centered at 374 and 434 nm, respectively. For H-BAS:Eu^{2+}, there are two possibilities for the origin of the emission peak at 374 nm. First, the emission wavelength of Eu^{2+}-activated phosphor was determined by the relationship between ^6P_j (here $j = 3/2$, 5/2, and 7/2) and the lowest 5d level and $^8S_{7/2}$.[18,19] For H-BAS:Eu^{2+}, the emission peak at 374 nm can be ascribed to transition of $^6P_{3/2}-^8S_{7/2}$ of Eu^{2+} ions because the position of the emission peak having a relative narrow shape was located in the
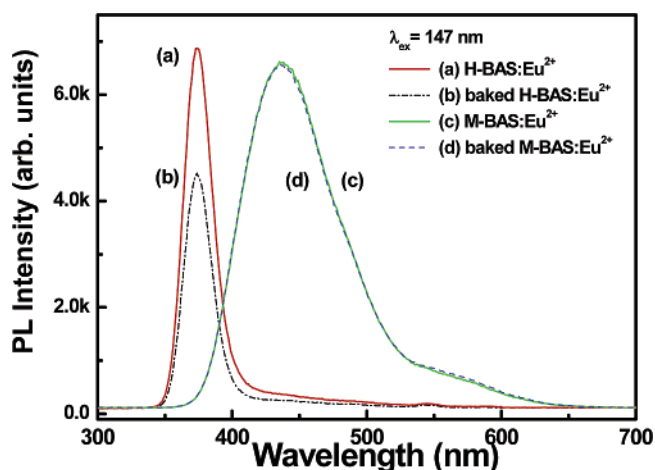

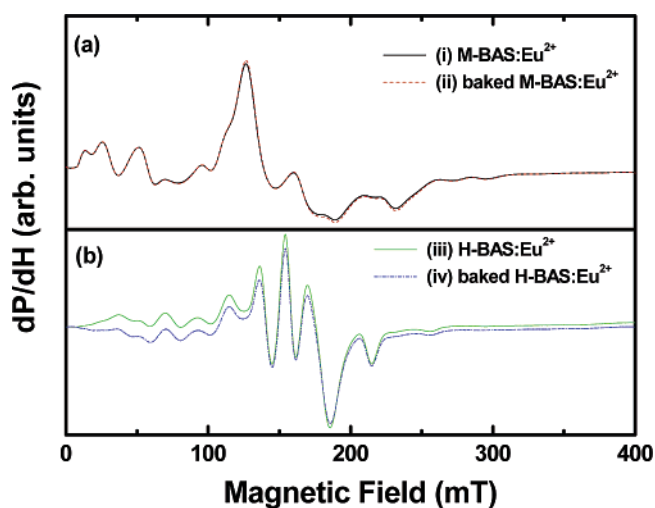**Figure 1.** PL spectra of polymorph BAS:Eu^{2+} before and after the baking process at 500 °C in air.

Figure 2. ESR spectra of polymorph BAS:Eu^{2+} before and after the baking process at 500 °C in air: (a) M-BAS:Eu^{2+}, (b) H-BAS:Eu^{2+}.

ultraviolet region. Second, it can be ascribed to 5d level splitting of Eu^{2+} ions in H-BAS.[20,21] That is, the lowest 5d level was located around $^6P_{3/2}$ by a weak crystal field. Considering both possibilities, the splitting of the 5d level of the Eu^{2+} in H-BAS was more reasonable than the transition of $^6P_{3/2}-^8S_{7/2}$ of Eu^{2+} ions because the emission spectrum of H-BAS:Eu^{2+} was too broad to be a 4f−4f transition.[18,19,22] On the other hand, for M-BAS:Eu^{2+}, owing to the strong crystal field around Eu^{2+} ions, the lowest 5d level would become lower than the $^6P_{7/2}$ level, and its emission peak was observed at 434 nm.

To investigate thermal stability, both M- and H-BAS:Eu^{2+} were baked at 500 °C in air, respectively. The PL intensity of H-BAS:Eu^{2+} was significantly reduced after the baking process, corresponding to a reduction of 34%. However, for M-BAS:Eu^{2+}, its PL intensity maintained the initial intensity of the fresh one. The decrease of PL intensity of H-BAS:Eu^{2+} can be attributed to either the lattice degradation or the decrease of the Eu^{2+} concentration.[1,6] If there is the lattice

(16) Larson, A. C.; Von Dreele, R. B. *Los Alamos Natl. Lab., [Rep.] LAUR* **1994**, *86*, 748.
(17) Finger, L. W.; Cox, D. E.; Jephcoat, A. P. *J. Appl. Crystallogr.* **1994**, *27*, 892.
(18) Shinoya, S., Yen, W. M., Eds. *Phosphor Handbook*; CRC Press: Boca Raton, FL, 1998.
(19) Blasse, G.; Grabmaier, B. C. *Luminescent Materials*; Springer-Verlag: New York, 1994.

(20) Laud, K. R.; Gibbons, E. F.; Tien, T. Y.; Stadler, H. L. *J. Electrochem. Soc.* **1971**, *118*, 918.
(21) Baby, T.; Nampoori, V. P. N. *Solid State Commun.* **1992**, *81*, 367.
(22) Ryan, F. M.; Lehmann, W.; Feldman, D. W.; Murphy, J. *J. Electrochem. Soc.* **1971**, *121* (11), 1477.

Table 1. Refined Structural Parameters for H-BAS:Eu²⁺ and M-BAS:Eu²⁺ Obtained from the Rietveld Refinement Using X-ray Powder Diffraction Data at Room Temperature[a]

atom	x	y	z	g^b	$100U_{iso}{}^c$ (Å²)
			H-BAS:Eu²⁺ [d]		
Ba	0.0	0.0	0.0	0.95[e]	0.0248(8)[f]
Eu	0.0	0.0	0.0	0.05[e]	0.0248(8)[f]
Al	1/3	2/3	0.28420(8)	1.0	0.0084(1)
Si	1/3	2/3	0.70479(7)	1.0	0.0204(6)
O(1)	1/3	2/3	0.50556(3)	1.0	0.0209(1)
O(2)	0.0056(3)	0.4462(9)	0.20953(1)	1.0	0.0166(6)
			M-BAS:Eu²⁺ [g]		
Ba	0.282 67(7)	0.001 37(4)	0.065 65(1)	0.95[e]	0.0073(8)[f]
Eu	0.282 67(7)	0.001 37(4)	0.065 65(1)	0.05[e]	0.0073(8)[f]
Si (1)	0.008 68(9)	0.183 45(5)	0.111 14(4)	1.0	0.0034(1)
Al(1)	0.008 43(4)	0.183 04(1)	0.614 64(6)	1.0	0.0050(7)
Al(2)	0.703 15(7)	0.121 93(1)	0.173 52(4)	1.0	0.0022(4)
Si (2)	0.707 94(3)	0.121 93(1)	0.173 52(4)	1.0	0.0086(5)
O(1)	−0.003 21(2)	0.140 86(1)	0.011 30(8)	1.0	0.0085(1)
O(2)	0.626 31(9)	−0.007 51(5)	0.144 75(6)	1.0	0.0109(6)
O(3)	0.829 96(7)	0.140 40(0)	0.112 03(7)	1.0	0.0028(1)
O(4)	0.822 86(6)	0.135 68(9)	0.614 63(8)	1.0	0.0126(2)
O(5)	0.026 48(5)	0.307 49(9)	0.121 14(1)	1.0	0.0002(3)
O(6)	0.026 25(5)	0.308 18(3)	0.631 29(1)	1.0	0.0029(8)
O(7)	0.188 12(0)	0.131 68(7)	0.197 25(7)	1.0	0.0049(2)
O(8)	0.191 77(8)	0.120 92(5)	0.699 94(7)	1.0	0.0066(1)

[a] The numbers in parentheses are the estimated standard deviations of the last significant figure. [b] Occupation factor. [c] Isotropic atomic displacement factor. [d] Space group: $P\bar{3}$ (No. 147); $a = 5.2955(9)$, $b = 5.2955(9)$, and $c = 7.78169(5)$ Å; $\alpha = 90$, $\beta = 90$, and $\gamma = 120°$. [e] Constraint on occupancy: $g(Ba) + g(Eu) = 1.0$. [f] Constraint on isotropic atomic displacement factor: $U_{iso}(Ba) = U_{iso}(Eu)$. [g] Space group: $I2/c$ (No. 15); $a = 8.626 82(7)$, $b = 14.040 98(5)$, and $c = 13.3935(7)$ Å; $\alpha = 90$, $\beta = 115.11(5)$, and $\gamma = 90°$.

degradation of H-BAS:Eu²⁺, the PL intensity of H-BAS:Eu²⁺ can be decreased because it is difficult to transfer the energy from the host lattice to the activator.[23] However, when compared the XRD patterns of fresh M- and H-BAS:Eu²⁺ with those of M- and H-BAS:Eu²⁺ baked at 500 °C in air, no impurity phase was found. This result indicates that the concentration change of Eu²⁺ ions against the outer oxidation atmosphere causes the PL intensity decrease of H-BAS:Eu²⁺.

The difference between the electronic configuration of the Eu²⁺ ion and that of Eu³⁺ exists: the Eu²⁺ ion has a paramagnetic property (4f⁷, S = 7/2, L = 0, J = 7/2), while the Eu³⁺ ion does not have it (4f⁶, S = 3, L = 3, J = 0).[1,13] Because ESR is able to distinguish whether there exist Eu²⁺ ions or not by responding to paramagnetic ions, ESR was used to observe the Eu²⁺ ion concentration of M- and H-BAS:Eu²⁺ before and after the baking process. The ESR spectra of M- and H-BAS:Eu²⁺ are shown in Figure 2. Although it is difficult to determine the g value of the Eu²⁺ ion from the ESR spectra as a result of its anisotropic properties, it is enough to qualitatively compare the concentration of Eu²⁺ ions in terms of peak intensity. In the ESR spectra of both fresh and baked M-BAS:Eu²⁺, all the peaks showed the same peak positions and shapes, and their intensities also were not changed as shown in Figure 2a. However, the ESR peak intensity of all peaks in the baked

Table 2. Selected Interatomic Distances and Bond Angles for M- and H-BAS:Eu²⁺ at Room Temperature

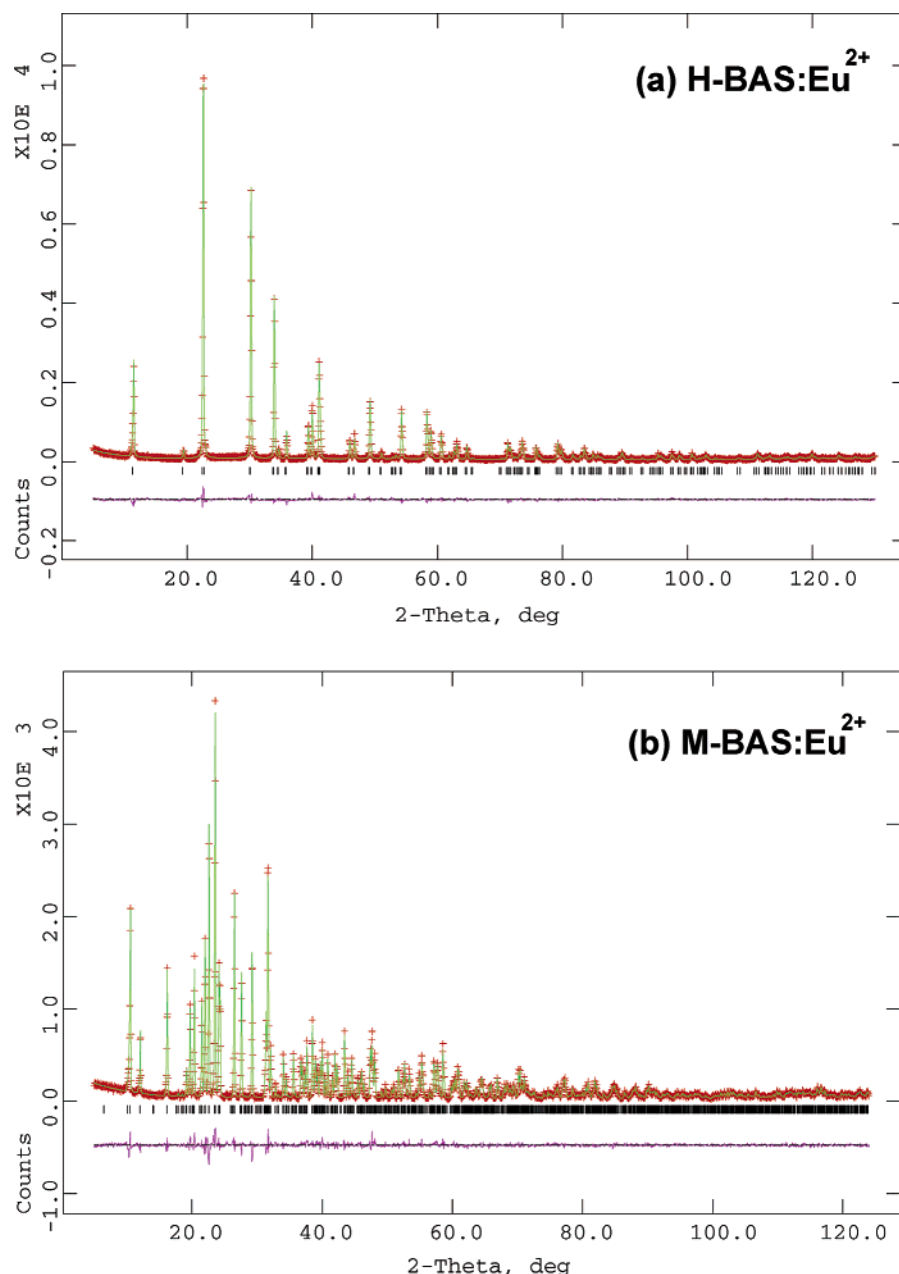| M-BAS:Eu²⁺				H-BAS:Eu²⁺			
distance (Å)		angle (deg)		distance (Å)		angle (deg)	
	tetrahedron coordination				tetrahedron coordination		
Si(1)−O(1)	1.503(1)	O(1)−Si(1)−O(3)	101.3(2)	Si(1)−O(1)	1.551(2)	O(1)−Si(1)−O(1)	112.8(1)
Si(1)−O(3)	1.646(1)	O(1)−Si(1)−O(5)	114.7(1)	Si(1)−O(2)	1.718(1)	O(1)−Si(1)−O(2)	112.8(1)
Si(1)−O(5)	1.625(2)	O(1)−Si(1)−O(7)	103.1(1)	Si(1)−O(2)	1.718(2)	O(1)−Si(1)−O(2)	112.8(1)
Si(1)−O(7)	1.661(1)	O(3)−Si(1)−O(5)	113.1(1)	Si(1)−O(2)	1.718(1)	O(2)−Si(1)−O(2)	105.9(1)
		O(3)−Si(1)−O(7)	115.7(2)			O(2)−Si(1)−O(2)	105.9(1)
		O(5)−Si(1)−O(7)	108.3(2)			O(2)−Si(1)−O(2)	105.8(2)
	tetrahedron coordination				tetrahedron coordination		
Si(2)−O(2)	1.573(2)	O(2)−Si(2)−O(4)	107.4(1)	Al(1)−O(1)	1.723(1)	O(1)−Al(1)−O(2)	110.7(2)
Si(2)−O(4)	1.584(2)	O(2)−Si(2)−O(6)	100.4(2)	Al(1)−O(2)	1.639(1)	O(1)−Al(1)−O(2)	110.7(2)
Si(2)−O(6)	1.721(1)	O(2)−Si(2)−O(8)	106.9(2)	Al(1)−O(2)	1.639(2)	O(1)−Al(1)−O(2)	110.7(2)
Si(2)−O(8)	1.639(1)	O(4)−Si(2)−O(6)	113.7(1)	Al(1)−O(2)	1.639(1)	O(2)−Al(1)−O(2)	108.1(1)
		O(4)−Si(2)−O(8)	115.8(2)			O(2)−Al(1)−O(2)	108.1(2)
		O(6)−Si(2)−O(8)	110.9(1)			O(2)−Al(1)−O(2)	108.1(1)
	tetrahedron coordination						
Al(1)−O(1)	1.877(1)	O(1)−Al(1)−O(4)	104.7(2)				
Al(1)−O(4)	1.715(2)	O(1)−Al(1)−O(6)	113.1(2)				
Al(1)−O(6)	1.647(1)	O(1)−Al(1)−O(8)	100.8(1)				
Al(1)−O(8)	1.737(1)	O(4)−Al(1)−O(6)	112.7(1)				
		O(4)−Al(1)−O(8)	113.6(2)				
		O(6)−Al(1)−O(8)	111.1(1)				
	tetrahedron coordination						
Al(2)−O(2)	1.796(2)	O(2)−Al(2)−O(3)	105.6(2)				
Al(2)−O(3)	1.691(2)	O(2)−Al(2)−O(5)	103.7(2)				
Al(2)−O(5)	1.662(1)	O(2)−Al(2)−O(7)	107.5(2)				
Al(2)−O(7)	1.696(1)	O(3)−Al(2)−O(5)	111.8(1)				
		O(3)−Al(2)−O(7)	112.5(2)				
		O(5)−Al(2)−O(7)	115.4(2)				
	9-coordinated polyhedron				12-coordinated polyhedron		
M[a]−O(1)	2.892(2)			M[a]−O(2)	3.369(1)		
M−O(1)	2.866(1)			M−O(2)	2.859(2)		
M−O(2)	2.689(2)			M−O(2)	2.859(2)		
M−O(3)	2.966(1)			M−O(2)	3.369(1)		
M−O(3)	2.937(2)			M−O(2)	3.369(1)		
M−O(5)	3.138(2)			M−O(2)	2.859(2)		
M−O(6)	3.157(2)			M−O(2)	2.859(2)		
M−O(7)	2.908(1)			M−O(2)	3.369(1)		
M−O(8)	2.861(1)			M−O(2)	3.369(1)		
				M−O(2)	2.859(2)		
				M−O(2)	2.859(2)		
				M−O(2)	3.369(1)		

[a] M: Ba or Eu.

Figure 3. Rietveld refinement patterns for polymorph BAS:Eu²⁺ X-ray powder diffraction data: (a) H-BAS:Eu²⁺, (b) M-BAS:Eu²⁺. The dot marks represent the observed intensities, and the solid line is the calculated one. A difference (obsd − calcd) plot is shown beneath. Tick marks above the difference data indicate the reflection positions.

H-BAS:Eu²⁺ was lower than that of the fresh H-BAS:Eu²⁺. It means that the valence state of Eu²⁺ ions is changed into that of Eu³⁺ ions because of the outer oxidation atmosphere. These results clarify that the crystal structure of M-BAS: Eu²⁺ is more resistant in protecting Eu²⁺ ions than that of H-BAS:Eu²⁺ from the outer oxidation atmosphere during the baking process.

The Rietveld refinement against XRD data was carried out to quantitatively confirm the sensitiveness of Eu²⁺ ions to the outer oxidation atmosphere. The structural models which approximate the actual structure for polymorph BAS: Eu²⁺ was constructed with crystallographic data on the basis of the hexagonal and monoclinic space groups $P\bar{3}$ and $I/2c$, respectively.[24,25] When Eu²⁺ ions are incorporated into the crystal structure of BAS, Eu²⁺ ions may substitute at all cationic sites, Ba²⁺, Al³⁺, and Si⁴⁺. However, considering

their respective ionic radii and allowed oxygen-coordination number (*n*), Al³⁺ (0.39 Å, *n* = 4), Si⁴⁺ (0.26 Å, *n* = 4), Ba²⁺ (1.42 Å, *n* = 8), and Eu²⁺ (1.25 Å, *n* = 8), it is difficult for Eu²⁺ ions to substitute for Al³⁺ or Si⁴⁺ ions.[26] Therefore, the structural refinement proceeded under the assumption that Eu²⁺ ions substituted for only Ba²⁺ ions. Consequently, the Rietveld refinement was carried out under the assumption that Eu²⁺ ions substituted for only Ba²⁺ ions. The occupancies of Eu²⁺ and Ba²⁺ sites were constrained so that both sites were fully occupied, and the total occupancy of the Eu²⁺ and Ba²⁺ ions was maintained at unity. The initial structural refinement cycles included the zero-point shift, the lattice parameters, the scale factor, and the background parameters as variables. Following satisfactory matching of peak positions, the atomic positions, the thermal parameters, and the peak profile parameters including the peak asymmetry were
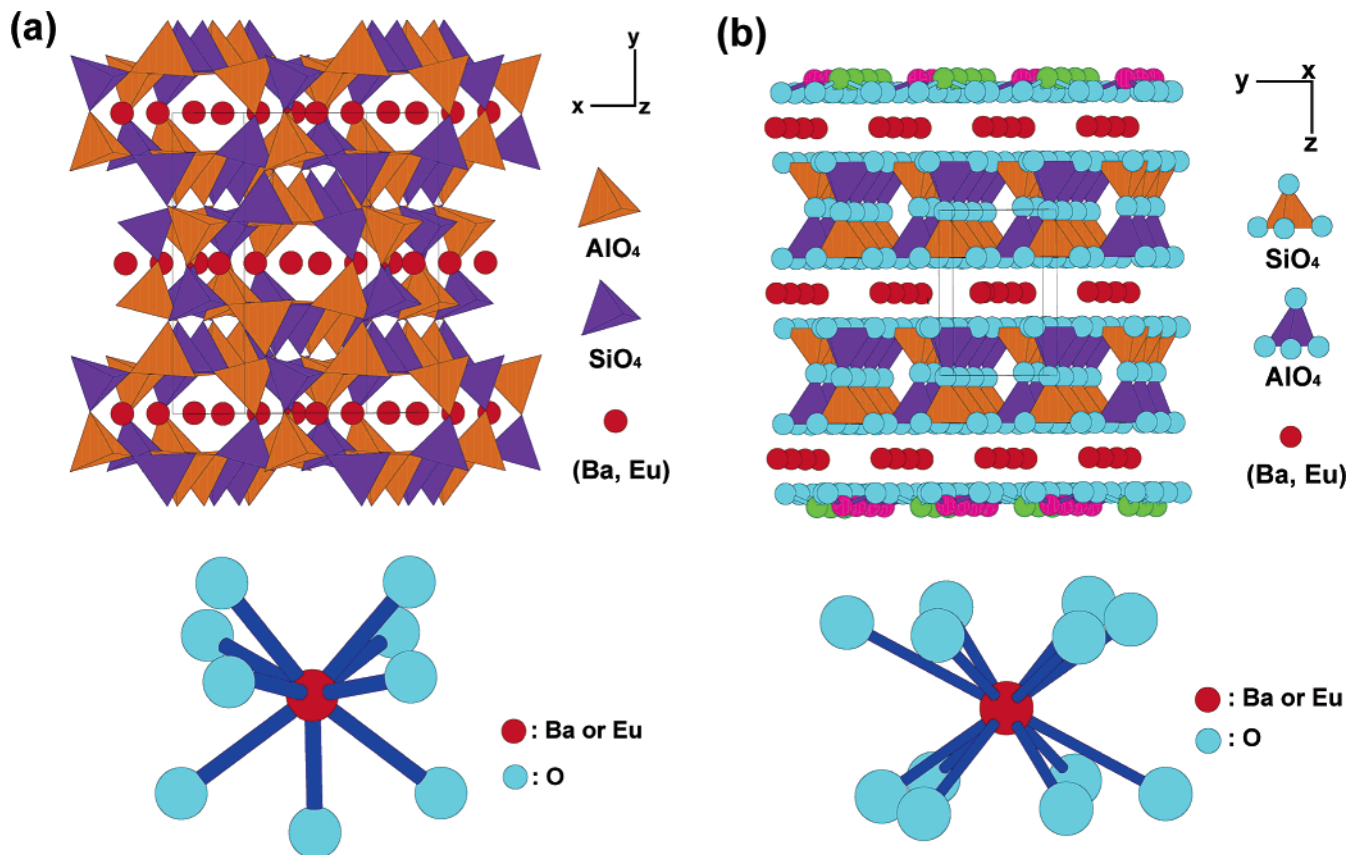
Figure 4. Crystal structures and cation polyhedra arrangements of polymorph BAS:Eu^{2+} phosphor: (a) M-BAS:Eu^{2+}, (b) H-BAS:Eu^{2+}.

refined. Si (NIST 640c) powder was used as an external standard to correct the zero-point shift for the measured diffraction data.

For H-BAS:Eu^{2+}, the final weighted R factor, R_{wp}, was 11.77%, and the goodness-of-fit indicator, S ($=R_{wp}/R_e$), was 1.515. For M-BAS:Eu^{2+}, R_{wp} was 11.36% and S was 1.355. The refined structural parameters, selected atomic distances, and bond angles of polymorph BAS:Eu^{2+} are listed in Tables 1 and 2, respectively. The structural parameters for polymorph BAS:Eu^{2+} were successfully determined by the Rietveld refinement using XRD data. Figure 3 shows Rietveld refinement results of H-BAS:Eu^{2+} and M-BAS:Eu^{2+}, respectively.

Figure 4 shows crystal structures and the coordination polyhedra of Eu^{2+} (or Ba^{2+}) ions surrounded by O^{2-} ions for M-BAS:Eu^{2+} and H-BAS:Eu^{2+}, respectively. As shown in Figure 4a, Eu^{2+} ions in M-BAS:Eu^{2+} having a space group $I/2c$ were tightly surrounded with each set of tetrahedral SiO$_4$ and AlO$_4$ units with the one above and below. That is, oxygen atoms form bridges between SiO$_4$ and AlO$_4$ tetrahedral. On the other hand, Eu^{2+} ions of H-BAS:Eu^{2+} with a space group $P\bar{3}$ occupied the sites sandwiched by the double layers as shown in Figure 4b, which correspond to the position of the open layer structure; that is, the Eu^{2+} ions of H-BAS:Eu^{2+} occupy the positions having the inversion symmetry between double sheets. As the difference in the crystal structure mentioned above, it is expected that Eu^{2+} ions of H-BAS:Eu^{2+} may be oxidized easily from the outer

oxidation atmosphere in comparison with those of M-BAS:Eu^{2+}.

The second of five general rules that Pauling proposed to build a stable crystal structure describes that the electrostatic strength of a bond is defined as follows:[27] If a positive ion with a charge of $+Z$ is surrounded by N negative ions in a coordination polyhedron, then the strength of the bonds from the cation to its anion neighbors is Z/N. As shown in Figure 4, M- and H-BAS:Eu^{2+} were constructed with coordination polyhedra consisting of Eu^{2+} ions surrounded by O^{2-} ions of 9- and 12-fold coordination, respectively. From Pauling's second rule, the $+2$ charge of Eu in M-BAS:Eu^{2+} must be equally divided among the surrounding O^{2-} ions of ninefold coordination, and the electrostatic strength of each bond is 0.222, while the electrostatic strength of Eu^{2+} ions surrounded by 12 oxygen ions in H-BAS:Eu^{2+} is 0.167. The difference in the electrostatic strength of the Eu^{2+} ions also indicates that Eu^{2+} ions of H-BAS:Eu^{2+} may be more susceptible to outer oxidation atmosphere than those of M-BAS:Eu^{2+}.

Furthermore, the average interatomic length was calculated to quantitatively confirm the sensitiveness of Eu^{2+} ions to the outer oxidation atmosphere using the Rietveld refinement against XRD data. The average interatomic length between Eu^{2+} and oxygen (d_{Eu-O}) in M-BAS:Eu^{2+} was 2.934(2) Å, while d_{Eu-O} of H-BAS:Eu^{2+} was 3.114(1) Å. The difference

(23) Youkosawa, N.; Sato, G.; Nakazawa, E. *J. Electrochem. Soc.* **2003**, *150* (9), H197.

(24) Kremenovic, A.; Norby, P.; Dimitrijevic, R.; Dondur, V. *Solid State Ionics* **1997**, *101*, 611.
(25) Griffen, D. T.; Ribbe, P. H. *Am. Mineral.* **1976**, *61*, 414.
(26) Shannon, R. D. *Acta Crystallogr., Sect. A* **1976**, *32*, 751.
(27) Pauling, L. *J. Am. Chem. Soc.* **1929**, *51*, 1010.

in d_{Eu-O} of the two crystal structures supports that the Eu^{2+} ions substituting the Ba^{2+} ions in H-BAS:Eu^{2+} may be more sensitive to the external environmental conditions such as temperature and oxidation atmosphere than those of the M-BAS:Eu^{2+} because d_{Eu-O} of H-BAS:Eu^{2+} is longer than that of M-BAS:Eu^{2+}. Consequently, the thermal stability of phosphors may be closely related to the crystal structures of host materials because the binding energy between Eu^{2+} and O^{2-} ions related with the coordination number and the mean interatomic distance depend on crystal structure.

4. Conclusions

The difference in thermal stability between M- and H-BAS:Eu^{2+} can be ascribed to both crystal structures and the average interatomic length between the Eu^{2+} ion and oxygen. This study suggests that the host lattice having a nonopened structure and the substitutional site to make d_{Eu-O} be short in the given host lattice should be considered as an important criterion for the selection of a host lattice showing thermal stability during the baking process. Consequently, if we would make a design blue phosphor for PDP application or demand thermal stability, the confirmation of a host lattice being a stable crystal structure for Eu^{2+} ions will be a very important criterion.

CM051894V